CDF/PUB/TOP/PUBLIC/10793

Measurement of Single Top Quark Production in 7.5 fb^{-1} of CDF Data Using Neural Networks

The CDF Collaboration
URL http://www-cdf.fnal.gov
(Dated: Mar 20, 2013)

We report a measurement of single top quark production in lepton plus jets final state using 7.5 fb^{-1} of $p\bar{p}$ collision data collected by CDF Run II experiment. We select events in the W + jets topology consistent with the signature of a charged lepton (electron or muon), large missing transverse energy ($\not\!\!E_T$) from the W boson decay and two or three jets, at least one of them is required to be identified as originating from a bottom quark. We use the new POWHEG Monte Carlo generator for single top signal samples in s-channel, t-channel and Wt-channel, which are generated at NLO accuracy, with an assumed top quark mass of 172.5 GeV/c^2. The Neural Network multivariate method is used to discriminate signal against comparatively large backgrounds. We measure a cross section of $3.04^{+0.57}_{-0.53}$pb (stat. + syst.) and set a lower limit $|V_{tb}| > 0.78$ at the 95% confidence level, assuming $m_t = 172.5$ GeV/c^2.

Preliminary Results for Winter 2012 Conferences

I. INTRODUCTION

In the Standard Model (SM), top quark can be produced via the strong interaction as a $t\bar{t}$ pair. It also allows for top quark to be produced through electroweak interaction as single top quark plus jets, which is referred to as single top process. There are three production modes: the t-channel $\sigma^{NNNLO_{approx}}_{t-\text{channel}} = 2.12 \pm 0.22$ pb, the s-channel $\sigma^{NNNLO_{approx}}_{s-\text{channel}} = 1.06 \pm 0.06$ pb, and the Wt production mode $\sigma^{NNNL0_{approx}}_{Wt-\text{channel}} = 0.22 \pm 0.08$ pb. These cross sections predictions were made with the assumption of a top quark mass $m_t = 172.5$ GeV/c^2[1] [12]. The three relevant processes of single top quark production considered in the current analysis are shown in Fig. 1. In this analysis we select events with W-boson only decaying leptonically and two or three jets as described in Sec. II. Since a small signal has to be be extracted from a huge amount of background events in order to have a significant result, multivariate methods which exploit a large number of characteristic quantities are used. In this analysis, neural networks are used to discriminate single top-quark events by employing the NeuroBayes®[2] package as described in Sec. IV.

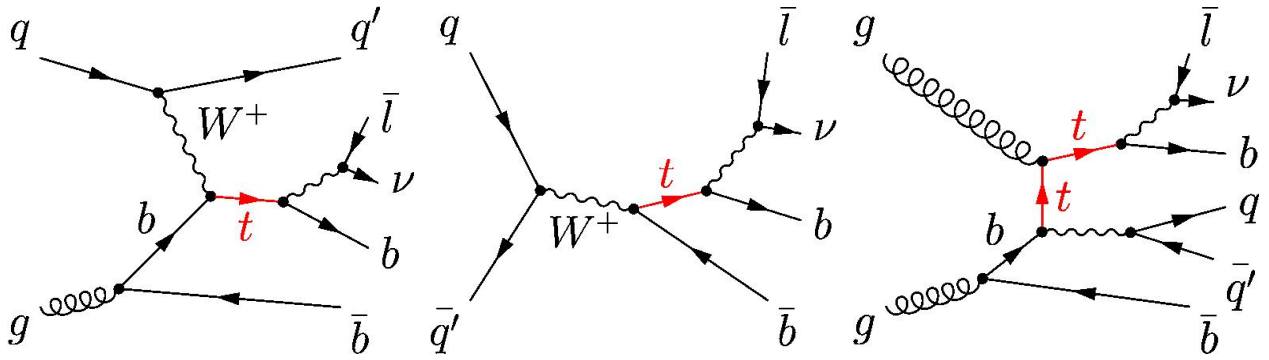

FIG. 1: Representative Feynman diagrams of single top-quark production channels: (a) t-channel $2 \to 3$ process at NLO with initial state gluon splitting, (b) s-channel at leading order, and (c) Wt associated production at NLO with initial state gluon splitting.

The single top was observed simultaneously by CDF and D0 experiments in 2009 [3][4] after almost 15 years of top quark discovery. It is still important for several reasons. Within the SM, the single-top signal allows for a direct measurement of the Cabibbo-Kobayashi-Maskawa(CKM) matrix element V_{tb}[5]. Furthermore, since the top quark decays before hadronization, its polarization can be directly observed in the angular correlations of its decay products[6][7]. Single top processes are expected to be sensitive to several kinds of new physics.
This note describes our analysis on electroweak production of single-top quarks using $p\bar{p}$ collision data collected at CDF II experiment up to March 2011, which correspond to a total integrated luminosity of 7.5 fb^{-1}.

II. DATA SAMPLE & EVENT SELECTION

The current analysis selects events in W + jets sample where the W-boson is required to decay leptonically, in order to reduce QCD background from multijets production. Therefore, the selected event has to be consistent with the signature of a charged lepton, large missing transverse energy $\not\!\!E_T$ plus two or three energetic jets. The lepton has to be single, isolated and with $p_T > 20$ GeV/c, while the $\not\!\!E_T$ has to be greater than 25 GeV. Furthermore, the $\not\!\!E_T$ is corrected for the presence of muons and jets. We accept Tight Lepton Candidates (TLC), which corresponds to the trigger categories of CEM, CMUP, CMX, PHX leptons, and Extended Muon Coverage (EMC) leptons, also called loose charged lepton candidates, which newly include ISOTRK. All these categories are orthogonal to each other. Jets are required to have corrected $E_T > 20$ GeV and $|\eta_{det}| < 2.8$ [13] in order to exploit the characteristic of forward topology of single top t-channel events. In order to improve the signal-background separation, we ask that at least one of the jets is identified as originated from a b-quark decay, using the `SecVtx` tagger.

A. Triggers

The data used for this analysis are collected from the high-p_T electron data stream, the high-p_T muon data stream, the high-p_T plug electron data stream and the high-$\not\!\!E_T$ data stream through March 2011. All these data correspond to a total integrated luminosity of 7.5 fb^{-1}. We select events from the datasets above which contain an energetic ($p_T > 20$ GeV/c) lepton. We apply turn-on curve correction to the Monte Carlo samples as described in [8] to account for some trigger inefficiencies in the low E_T range and for central values of η.

B. Event Selection

1. Lepton Selection

For each lepton category, we select events consistent with the topology of a W-boson decay plus two or three energetic jets. The W-boson events are selected by requiring a single, charged lepton with $E_T(p_T) > 20$ GeV/c and $|\eta| < 1.6$. We distinguish between tight and loose lepton candidates. The aim is to gain as much acceptance as possible. This is of the out most importance for muons, as we can recover the losses in the cracks of the μ coverage by adding the ISOTRK category.
We also apply the topological requirement of isolation to tight leptons: E_T not assigned to the lepton within cone size $R < 0.4$ in the lepton direction is $< 10\%$ of the lepton E_T. This requirement is not applied to loose leptons. For tight central electrons (CEM), tight plug electrons (PHX) and central muons (CMUP, CMX), we use the same event selection as detailed in $t\bar{t}$ cross section measurement [9].
In order to reduce various sources of backgrounds, several requirements are applied:
Dilepton Veto requires that an event must contain exactly one lepton and those contain more than one lepton are rejected. This veto rejects events in which $t\bar{t}$ decays into dilepton as well as diboson events.
Z boson Veto is implemented to avoid events containing a Z boson. We check that the lepton, paired with an opposite-signed high-p_T track, does not form an invariant mass $M_{\mathrm{l,track}}$ consistent with $76 \leq M_Z \leq 106$ GeV/c^2.
z Vertex cut requires the reconstructed primary z vertex of the event to be within a range of ± 60 cm with respect to the center of the detector.
Cosmic Veto remove event tagged as cosmic rays. This requirement is relevant for muons, since highly energetic muons can be created in the upper atmosphere and then penetrate through detectors. It is not applied to MC events because cosmic rays are not simulated.

2. Missing Transverse Energy

The presence of the neutrino coming from W-boson decay is estimated from the missing-transverse-energy ($\not\!\!E_T$) present in the event. We require $\not\!\!E_T > 25$ GeV for all lepton categories, corrected for the presence of muons (including muon-like isolated tracks) and Jet Energy Scale (JES).

3. Jet Reconstruction and Selection

The jets are identified using the JetClu algorithm with a cone size of 0.4. The jet energy is corrected up to level 5. At this level, the correction is for the η-dependence of the calorimeter response, for multiple $p\bar{p}$ interactions and absolute energy scale (including the underlying events). Tight jets are required to have corrected $E_T > 20$ GeV and $|\eta_{det}| < 2.8$ in order to exploit the characteristic of forward topology of single top events. Only events with exactly two or three tight jets are accepted. Moreover, in the final selection we also require one or two jets to be b-quark tagged (b-tagged) by requiring a displaced secondary vertex reconstructed by the Secvtx algorithm.

C. Rejection of QCD background

An important fraction of the background for W + jets final state processes comes from the QCD-multijets events which do not contain a W boson (they are also dubbed "non-W" or "QCD" events), but faking a W-boson-like signature. Those events are misidentified when one jet is mistaken as a high-p_T lepton and $\not\!\!E_T$ is generated from jet energy mis-measurement. Despite the low probability of such occurrences, the large number of multijets events

make this process an unavoidable background. In this case, the $\vec{\not\!\!E}_T$ often points to the lepton candidate direction. Thus we would expect small $\not\!\!E_T$ and small values for the angle $\Delta\phi(\vec{\not\!\!E}_T, jet)$. The procedure called "Single-Top QCD Veto" (STQCDVeto) is designed to reject this multijet background events. It mainly relies on the use of M_T^W and the variable MET-significance ($\not\!\!E_{T\,\mathrm{sig}}$). The MET-significance is defined as:

$$\not\!\!E_{T\,\mathrm{sig}} = \frac{\not\!\!E_T}{\sqrt{\sum_{\mathrm{jets}} C_{\mathrm{JES}}^2 \cos^2\left(\Delta\phi_{\mathrm{jet},\vec{\not\!\!E}_T}\right) E_{T,\mathrm{jet}}^{\mathrm{raw}} + \cos^2\left(\Delta\phi_{\vec{E}_{T,\mathrm{uncl}},\vec{\not\!\!E}_T}\right) \sum E_{T,\mathrm{uncl}}}} \tag{1}$$

where C_{JES} is the jet energy correction factor, $E_{T,\mathrm{jet}}^{\mathrm{raw}}$ is a jet's energy before corrections are applied, $\vec{E}_{T,\mathrm{uncl}}$ refers to the vector sum of the transverse components of calorimeter energy deposits not included in any reconstructed jets, and $\sum E_{T,\mathrm{uncl}}$ is the scalar sum of these unclustered energies.

Events passing the electron trigger must have $M_T^W > 20$ GeV. For CEM electrons, we require $\not\!\!E_{T\,\mathrm{sig}} > 3.5 - 0.05 M_T^W$ and additionally $\not\!\!E_{T\,\mathrm{sig}} > -7.6 + 3.2|\Delta\phi(l, \mathrm{jet})|$ in the 1-jet bin and $\not\!\!E_{T\,\mathrm{sig}} > 2.5 - 3.125|\Delta\phi(\mathrm{jet}_2, \not\!\!E_T)|$ in the 2-jets and 3-jets bins, where jet_2 is the second most energetic jet. Forward electrons PHX must have $\not\!\!E_{T\,\mathrm{sig}} > 2.0$ and $\not\!\!E_T > 45 - 30|\Delta\phi(\mathrm{jet}, \not\!\!E_T)|$ for the two leading jets in event. Tight muons CMUP and CMX must have $M_T^W > 10$ GeV, while for CMUP it is additionally required $\not\!\!E_T > -145 + 60|\Delta\phi(l, \mathrm{jet})|$ in the 1-jet bin. For the EMC the cut on $W-$boson transverse mass is raised from 10 GeV to 20 GeV in order to better reject QCD contamination.

D. Monte Carlo Signal and Background samples

The single top signal samples used in the current analysis are modeled using parton-level events generated by POWHEG and showered by PYTHIA, with a top mass set to 172.5 GeV/c^2. POWHEG interfaces NLO calculations with parton shower generators and produces parton-level events with positive (constant) weight at NLO accuracy. The use of POWHEG signal samples avoids the procedure of t-channel matching used in the previous single top analysis and permits the inclusion of Wt-channel in this analysis [10].
The background models are composed by different components. The W and Z plus light-flavor and heavy-flavor jet processes are modeled using ALPGEN version 2.10 showered with PYTHIA. The rest of the background processes, including the $t\bar{t}$, WW, WZ, and ZZ processes were generated using PYTHIA. For backgrounds involving a top quark, the top mass was set to 172.5 GeV/c^2. The production cross section and branching ratio of single top and major backgrounds are listed in Tab. I.

EW Processes	Theoretical Cross Section (pb)
$t\bar{t}$	7.3 ± 0.6
Single Top (s-ch)	1.0 ± 0.1
Single Top (t-ch)	2.1 ± 0.2
Single Top (Wt-ch)	0.2 ± 0.1
WW	11.3 ± 0.7
WZ	3.2 ± 0.2
ZZ	1.2 ± 0.1
Z + jets	787 ± 85

TABLE I: The theoretical cross sections and branching ratios used for MC-based processes. The cross sections are calculated at NLO assuming a top-quark mass of 172.5 GeV/c^2. BR depends on how samples are generated: some of them are generated inclusively with all decay modes and we use the unity for BR, some other exclusively with leptonic decays and we use the leptonic BR.

III. EVENT YIELD ESTIMATES

The contributions from the following individual backgrounds are calculated: falsely b-tagged events, W production with heavy-flavor quark pairs, QCD events with false W signatures, top quark production, and diboson production.

We estimate the amount of falsely b-tagged events (mistags) from the number of pretag W + light flavor events. The amount of pretag W + light flavor is determined by a fit of the pretag $\not\!\!E_T$ distribution to W and non-W templates. To estimate the amount of W + light flavor in the tagged sample, we apply a per-jet false tag rate parameterization (mistag matrix) to the pretag W + light flavor events. The mistag matrix is obtained from inclusive jet data.

The number of events from W + heavy flavor is calculated using information from both data and Monte Carlo samples. We calculate the fraction of W events with associated heavy flavor production in the ALPGEN samples. This fraction and the tagging efficiency of these events are applied to the number of events in the W + jets sample originated from data after correcting for the $t\bar{t}$ and electroweak contributions.

We use the $\not\!\!E_T$ shape difference between the non-W and the other background models to constrain the amount of QCD events. We perform a likelihood fit to the $\not\!\!E_T$ distribution to determine the total amount of QCD. We deduce the QCD fraction in the signal region by integrating the fitted distributions above our $\not\!\!E_T$ cut (25 GeV). We estimate the non-W contribution to the tagged sample by fitting the $\not\!\!E_T$ distribution of the tagged events. The prediction is showed in Tab. II.

Process	W+2jets, 1 tag	W+3jets, 1 tag	W+2jets, 2 tag	W+3jets, 2 tag
$t\bar{t}$	474 ± 49	1067 ± 109	98 ± 14	284 ± 42
WW	148 ± 21	48 ± 7	1.1 ± 0.3	1.2 ± 0.3
WZ	53 ± 6	14 ± 2	8.8 ± 1.3	2.4 ± 0.4
ZZ	1.7 ± 0.2	0.7 ± 0.1	0.3 ± 0.0	0.1 ± 0.0
Z+Jets	118 ± 15	46 ± 6	4.8 ± 0.7	2.7 ± 0.4
Wbb	1452 ± 437	434 ± 131	183 ± 56	65 ± 20
Wcc	766 ± 233	254 ± 77	10 ± 3	7 ± 2
Wcj	583 ± 177	128 ± 39	7.8 ± 2.4	3.5 ± 1.1
W+Mistags	1459 ± 148	433 ± 47	7.4 ± 1.5	5.4 ± 1.1
Non-W	316 ± 126	141 ± 57	6.8 ± 3.5	3.4 ± 3.2
t-channel	193 ± 25	84 ± 11	6 ± 1	15 ± 2.4
s-channel	128 ± 11	43 ± 4	32 ± 4	12 ± 1.6
Wt-channel	16 ± 4	26 ± 7	0.7 ± 0.2	2.3 ± 0.6
Total Prediction	5707 ± 877	2719 ± 293	367 ± 66	403 ± 53
Observed	5533	2432	335	355

TABLE II: Summary of the predicted numbers of signal and background events in the 2-jets and 3-jets samples, with systematic uncertainties on the cross section and Monte Carlo efficiencies included.

IV. NEURAL NETWORK DISCRIMINANT

The measurement of single top quark cross section present substantial experimental challenges comparing with $t\bar{t}$ production. It suffers from lower SM production rate and a large kinematically similar background. Simply counting events which pass our selection requirements will not yield a precise measurement of the single top cross section no matter how much data are accumulated. Further separation of the signal from backgrounds is required. In this analysis, we use artificial neural networks NeuroBayes®package to separate signal from background events.

The output distributions of s-, t-and Wt-channel events are combined into one signal distribution, where the ratio between them is set as predicted by the SM. We combine the background processes whose output distributions look similar and are hence difficult to distinguish. On this account, some of the processes are merged into one template with a ratio given by the background estimation. In total six background templates remain: $t\bar{t}$, W + heavy flavor, W + light flavor, diboson, Z + jets, and QCD.

The variables used in each network are summarized in Tab. III. Descriptions of the variables are listed follow. And some validation plots are listed in Figure IV–IV.

- $M_{\ell\nu b}$: The reconstructed top quark mass.
- $M_{\ell\nu bb}$: The reconstructed mass of the charged lepton, the neutrino, and the two b-tagged jets in the event.

TABLE III: Summary of variables used in the different neural networks in this analysis. Explanations of the variables are given in the text.

	2-jet		3-jet	
variable	1-tag	2-tag	1-tag	2-tag
$M_{\ell\nu b}$	✓	✓	✓	
$M_{\ell\nu bb}$		✓		✓
$M_{\mathrm{t}}^{\ell\nu b}$	✓	✓	✓	✓
M_{jj}	✓	✓	✓	✓
M_{t}^{w}	✓	✓		
$E_{\mathrm{t}}^{b_{\mathrm{top}}}$		✓	✓	
$E_{\mathrm{t}}^{b_{\mathrm{other}}}$				✓
$\sum e_{\mathrm{t}}^{jj}$			✓	✓
$E_{\mathrm{t}}^{\mathrm{light}}$	✓			✓
p_{t}^{ℓ}	✓			
$p_{\mathrm{t}}^{\ell\nu jj}$			✓	✓
H_{t}	✓		✓	
$\not\!\!E_T$		✓		
$\not\!\!E_{T\,\mathrm{sig}}$			✓	
$\cos\theta_{\ell j}$	✓		✓	✓
$\cos\theta_{\ell w}^{w}$	✓			
$\cos\theta_{\ell w}^{t}$	✓			
$\cos\theta_{jj}^{t}$		✓		✓
$Q\times\eta$	✓		✓	✓
η_{ℓ}		✓		
η_{w}	✓	✓		
$\sum\eta_j$	✓		✓	
$\Delta\eta_{jj}$			✓	✓
$\Delta\eta_{t,\mathrm{light}}$			✓	
$\sqrt{\hat{s}}$				✓
Centrality				✓
Jet flavor separator	✓	✓	✓	

- $M_{\mathrm{T}}^{\ell\nu b}$: The transverse mass of the reconstructed top quark.
- M_{jj}: The invariant mass of the two jets. In the three-jet networks, all combinations of jets are included as variables.
- M_{T}^{W}: The transverse mass of the reconstructed W boson.
- $E_{\mathrm{T}}^{b_{\mathrm{top}}}$: The transverse energy of the b quark from top decay.
- $E_{\mathrm{T}}^{b_{\mathrm{other}}}$: The transverse energy of the b quark not from top decay.
- $\sum E_{\mathrm{T}}^{jj}$: The sum of the transverse energies of the two most energetic jets. In the 3-jets 1-tag network, all combinations of two jets are used to construct separate $\sum E_{\mathrm{T}}^{jj}$ input variables.
- E_{T}^{light}: The transverse energy of the untagged or lowest-energy jet.
- p_{T}^{ℓ}: The transverse momentum of the charged lepton.
- $p_{\mathrm{T}}^{\ell\nu jj}$: The magnitude of the vector sum of the transverse momentum of the charged lepton, the neutrino, and all the jets in the event.
- H_{T}: The scalar sum of the transverse energies of the charged lepton, the neutrino, and all the jets in the event.
- $\not\!\!E_T$: The missing transverse energy.
- $\not\!\!E_{T\,\mathrm{sig}}$: The significance of the missing transverse energy $\not\!\!E_T$

- $\cos\theta_{\ell j}$: The cosine of the angle between the charged lepton and the untagged or lowest-energy jet in the top quark's reference frame.
- $\cos\theta^{W}_{\ell W}$: The cosine of the angle between the charged lepton and the reconstructed W boson in the W boson's reference frame.
- $\cos\theta^{t}_{\ell W}$: The cosine of the angle between the charged lepton and the reconstructed W boson in the top quark's reference frame.
- $\cos\theta^{t}_{jj}$: The cosine of the angle between the two most energetic jets in the top quark's reference frame.
- $Q \times \eta$: The charge of the lepton multiplied by the pseudorapidity of the untagged jet.
- η_{ℓ}: The pseudorapidity of the charged lepton.
- η_{W}: The pseudorapidity of the reconstructed W boson.
- $\sum \eta_{j}$: The sum of the pseudorapidities of all jets.
- $\Delta\eta_{jj}$: The difference in pseudorapidity of the two most energetic jets. In the three-jet two-tag network, the difference between the two least energetic jets is also used.
- $\Delta\eta_{t,\mathrm{light}}$: The difference in pseudorapidity between the untagged or lowest-energy jet and the reconstructed top quark.
- $\sqrt{\hat{s}}$: The energy of the center-of-mass system of the hard interaction, defined as the $\ell\nu b$ system plus the recoiling jet.
- Centrality: The sum of the transverse energies of the two leading jets divided by $\sqrt{\hat{s}}$.
- b_{NN}: The jet flavor separator neural network output. For two-tag events, the sum of the two outputs is used.

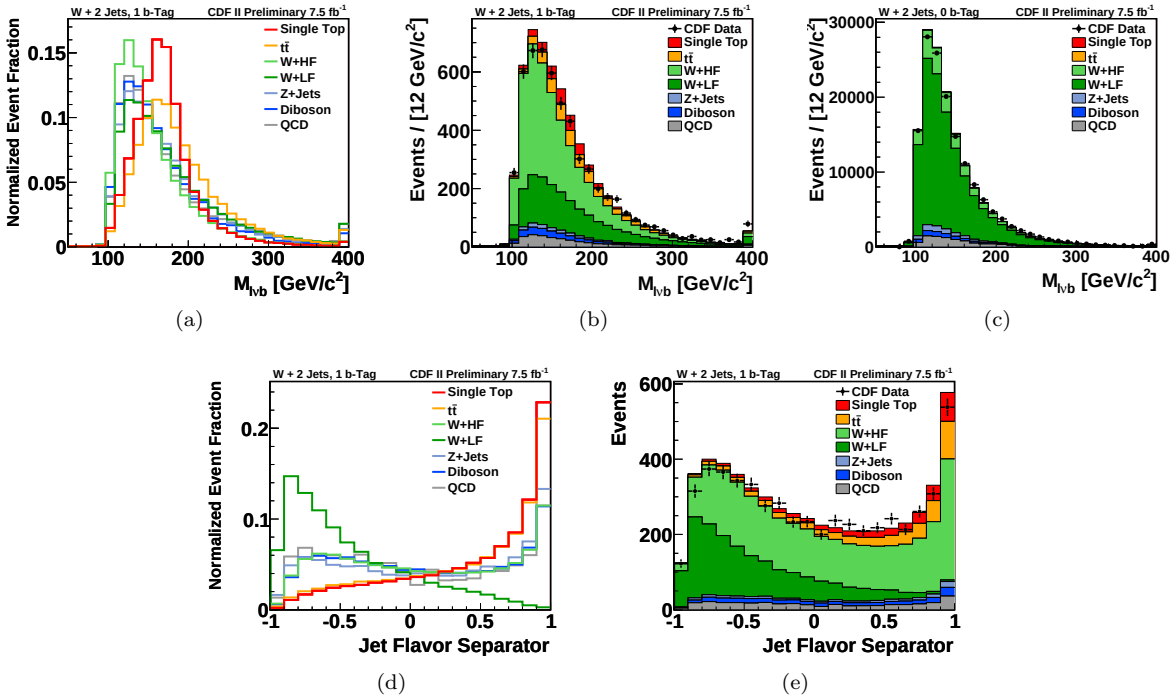

FIG. 2: Shape comparison (first column) and MC modeling validation (second column) in the 2-jets 1-tag signal region, and MC modeling validation (third column) in the untagged 2-jet sideband of the discriminating input-variables for TLC events. For jet flavor separator, such value doesn't exist for untagged events.

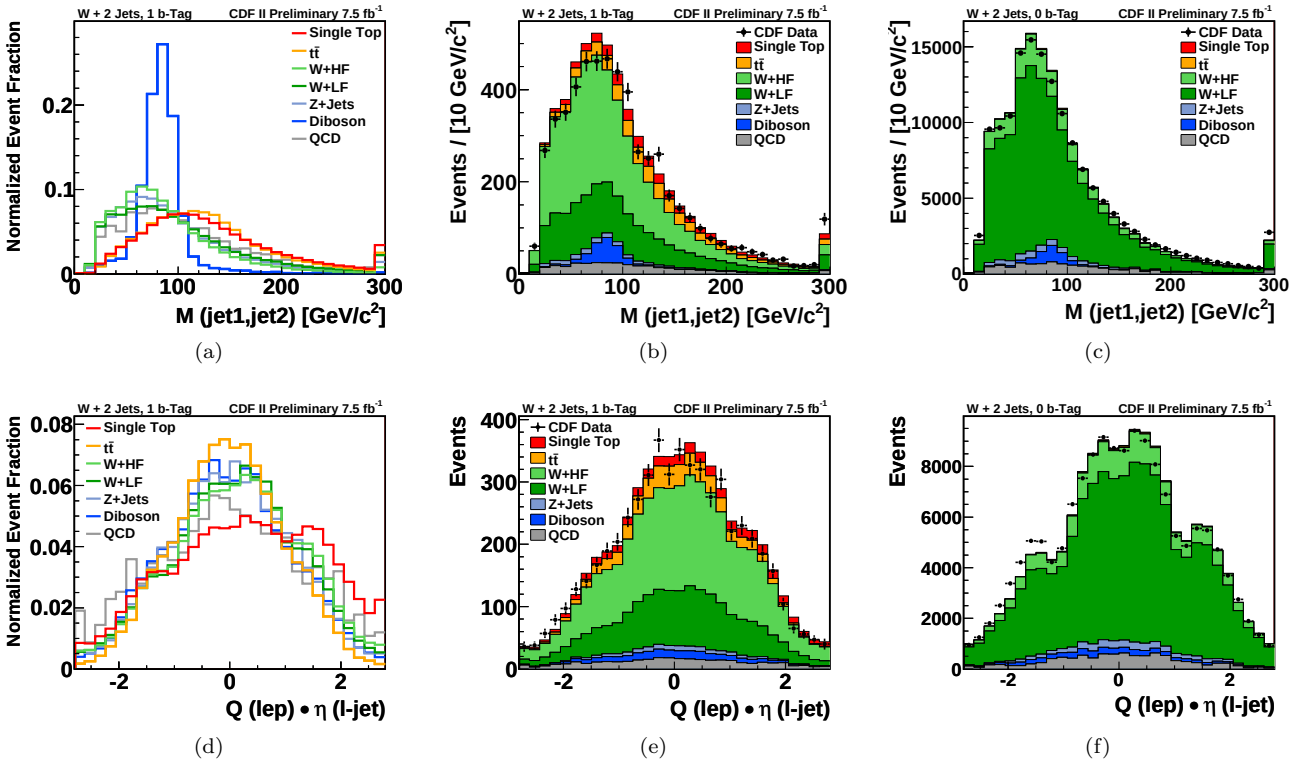

FIG. 3: Shape comparison (first column) and MC modeling validation (second column) in the 2-jets 1-tag signal region, and MC modeling validation (third column) in the untagged two-jet sideband of the discriminating input-variables for TLC events.

To optimize the NN performers, in the 2-jets 2-tag channel, we train on s-channel as signal while t- and Wt-channel treated as background like. We train on t-channel in the rest jet and tag channels. To further improve our cross section measurement, we studied the NN training with systematics-mixed sample in our NN training process. By including the jet energy scale shifted samples and Q^2 varied samples, our studies shows that we can expect about 3% improvement on the uncertainty of cross section measurement. We use this technique in our final NN training.

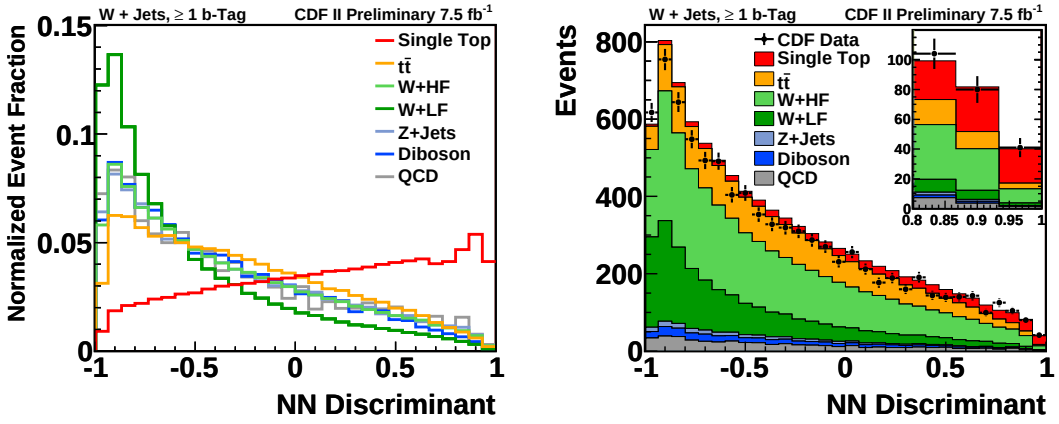

FIG. 4: Signal and background templates in the 2-and 3-jets signal region.

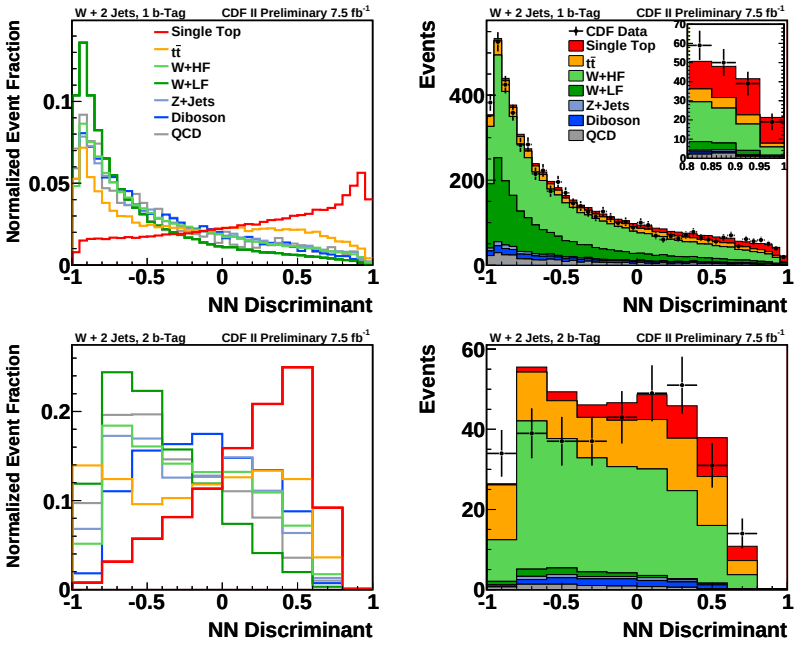

FIG. 5: Signal and background templates in the 2-jets signal region.

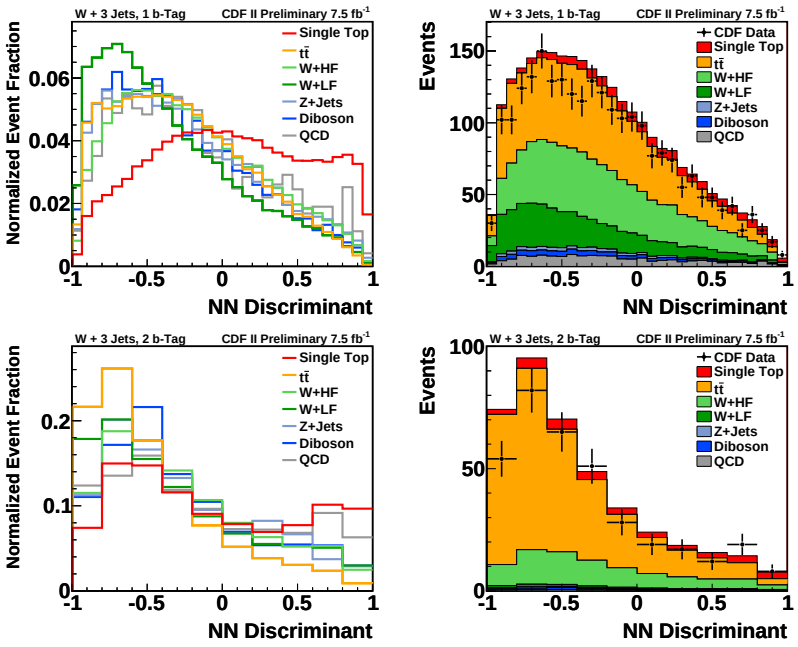

FIG. 6: Signal and background templates in the 3-jets signal region.

V. SYSTEMATIC UNCERTAINTIES

The measurement of the single top cross section requires substantial input from theoretical models, Monte Carlo simulations, and extrapolations from control samples in data. We assign systematic uncertainties to our predictions and include the effects of these uncertainties on the measured cross section. The systematic uncertainties we consider are mostly the same as the previous analysis [11]. We consider three categories of systematic uncertainty: uncertainty in the predicted rates of the signal and background processes, uncertainty in the shapes of the distribution of the discriminant variables, and uncertainty arising from the limited number of Monte Carlo events used to predict the signal and background expectations in each bin of each discriminant distribution.

As in the previous analysis [11], checks of the untagged W + 2 jets control region show that the rate of appearance of jets at high $|\eta|$ in the data is underestimated by the prediction. Inaccurate modelling of the distribution of this variable has a potentially significant impact on the analysis because of use of the sensitive variable $Q\times\eta$ as in Fig. 3(f). Similarly, we observed a mis-modelling in the distribution of $\Delta R(j_1, j_2) = \sqrt{(\Delta\eta)^2 + (\Delta\phi)^2}$. With recent studies at CDF, we found out that the mismodelling of the jet η and ΔR mainly comes from W + light flavor events. We choose to reweight only W + light flavor process as a systematic uncertainty. The weighting factor is based on the ratio of the data and Monte Carlo in the untagged sideband by three iterations of comparisons of $E_T(j_1, j_2)$, $\eta(j_1, j_2)$ and $\Delta R(j_1, j_2)$.

TABLE IV: Sources of systematic uncertainty considered in this analysis.

Source of Uncertainty	Rate	Shape	Processes affected
Jet energy scale	0–8%	X	all
Initial and final state radiation	0–6%	X	single top, $t\bar{t}$
Parton distribution functions	0–1%	X	single top, $t\bar{t}$
Acceptance and efficiency scale	1–7%		single top, $t\bar{t}$, diboson, Z/γ^*+jets
Luminosity	6%		single top, $t\bar{t}$, diboson, Z/γ^*+jets
Jet flavor separator		X	all
Mistag model		X	W+light
Non-W model		X	Non-W
Factorization and renormalization		X	$Wb\bar{b}$
Jet η and ΔR distribution		X	W+light
Non-W normalization	40%		Non-W
$Wb\bar{b}$ and $Wc\bar{c}$ norm	30%		$Wb\bar{b}$, $Wc\bar{c}$
Wc normalization	30%		Wc
Mistag normalization	10–20%		W+light
$t\bar{t}$ normalization	8%		$t\bar{t}$
Monte Carlo generator	3–7%		single top, $t\bar{t}$
Single top normalization	7%		single top
Top mass	2-12%	X	single top, $t\bar{t}$

∗ X indicates the sources of uncertainty from shape variation
∗ Sources listed below double line are used only in $|V_{tb}|$ measurement

VI. MEASUREMENT

The measurement of single top-quark cross section is performed using the standard CDF MClimit package. The handling of the systematic uncertainties is Bayesian, in that priors are assigned for the values of the uncertain nuisance parameters. The impacts of the nuisance parameters on the predictions are evaluated, and integrals are performed over the values of the nuisance parameters. Since the single top signal template and the $t\bar{t}$ background template are functions of m_t, we quote the single top quark and $t\bar{t}$ cross section assuming a top quark mass $m_t = 172.5$ GeV/c^2. We do not include the rate uncertainty on the top quark mass when measuring the cross section.

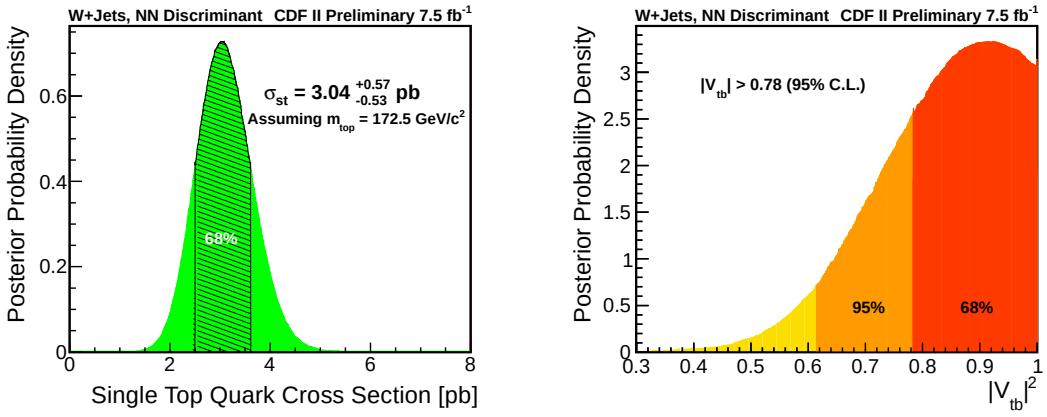

(a) (b)

FIG. 7: The posterior curve of the cross section measurement calculated with the super discriminant histograms as inputs (a), the posterior curve for the $|V_{tb}|$ calculation (b).

A. Cross Section Measurement

We measured the total cross section of single top quark production σ_{st}, assuming the SM ratio among s-, t and Wt-channel production: $\beta_s = \beta_t = \beta_{Wt} \equiv \beta$. The posterior distribution is shown in Figure 7(a). From this distribution, we obtain a single top quark cross section measurement of $\sigma_{st} = 3.04^{+0.57}_{-0.53}$ pb, assuming a top quark mass of 172.5 GeV/c^2.

B. Extraction of Bounds on $|V_{tb}|$

To extract $|V_{tb}|$ from the combined measurement, we take advantage of the fact that the production cross section σ_{st} is directly proportional to $|V_{tb}|^2$. We use the relation

$$|V_{tb}|^2_{\text{measured}} = \sigma_{st}^{\text{measured}} |V_{tb}|^2_{\text{SM}} / \sigma_{st}^{\text{SM}}, \tag{2}$$

where $|V_{tb}|^2_{\text{SM}} \approx 1$ and $\sigma_{st}^{\text{SM}} = 3.4 \pm 0.36$. Equation 2 further assumes that $|V_{tb}|^2 \gg |V_{ts}|^2 + |V_{td}|^2$, because we are assuming that the top quark decays to Wb 100% of the time, and because we assume that the production cross section scales with $|V_{tb}|^2$, while the other CKM matrix elements may contribute as well if they were not very small. Figure 7(b) shows the joint posterior distribution of all of our independent channels as a function of $|V_{tb}|^2$ (which includes the theoretical uncertainty on the predicted production rate, which is not part of the cross section posterior), from which we obtain a 95% confidence level lower limit of $|V_{tb}| > 0.78$ and extracted $|V_{tb}| = 0.96 \pm 0.09(\text{stat.} + \text{syst.}) \pm 0.05(\text{theory})$.

C. Two-Dimensional Fit Results

The extraction of the combined signal cross section σ_{st} proceeds by constructing a one-dimensional Bayesian posterior with a uniform prior in the cross section to be measured. An extension of this is to form the posterior in the two-dimensional plane, σ_s vs. σ_{t+Wt}, and to extract the s-channel and the t- and Wt-channel cross sections separately. Here we combined the Wt-channel with t-channel due to the small predicted cross section of Wt-channel at Tevatron and the similar final state signature with t-channel. In addition, this analysis doesn't sensitive to the Wt-channel process. Our studies show that the Wt-channel contributes negligible effects in this two-dimensional fit. Thus we will hereby neglect the $Wt-$channel contribution in the later extraction.

The best-fit cross section is the one for which the posterior is maximized, and corresponds to $\sigma_s = 1.81^{+0.63}_{-0.58}$ pb and $\sigma_t = 1.49^{+0.47}_{-0.42}$ pb. The uncertainties on the measurements of σ_s and σ_t are correlated with each other because s-channel and t-channel signals both populate the signal-like bins of each of our discriminant variables. Regions of 68.3%, 95.5%, and 99.7% credibility are derived from the distribution of the posterior by evaluating the smallest

region in area that contains 68.3%, 95.5% or 99.7% of the integral of the posterior. The best-fit values, the credibility regions, and the SM predictions of σ_s and σ_t are shown in Figure 8. We compare these with the NNNLO predictions of $\sigma_{t+Wt} = 2.34 \pm 0.3$ pb and $\sigma_s = 1.06 \pm 0.06$ pb [1].

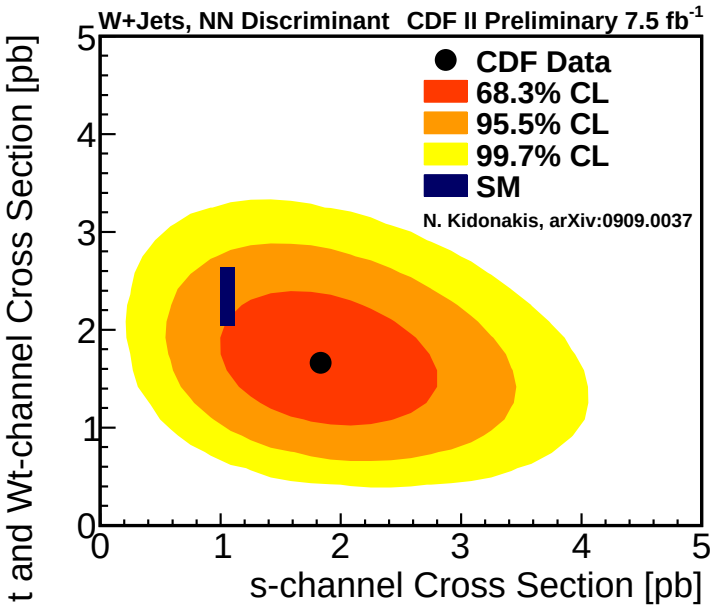

FIG. 8: The results of the two-dimensional fit for σ_s and σ_{t+Wt}. The black point shows the best fit value, and the 68.3%, 95.5%, and 99.7% credibility regions are shown as shaded areas. The SM predictions are also indicated with their theoretical uncertainties.

VII. CONCLUSIONS

We presented a measurement of single top quark production in lepton plus jets final state using 7.5 fb^{-1} of $p\bar{p}$ collision data collected by CDF II experiment. We select events in the W + jets topology consistent with the signature of a charged lepton (electron or muon), large missing transverse energy ($\not\!\!E_T$) from the W boson decay and two or three jets, at least one of them is required to be identified as originating from a bottom quark. We use the new POWHEG Monte Carlo generator for single top signal samples in s-channel, t-channel and Wt-channel, which are extended at NLO accuracy, with an assumed top quark mass of 172.5 GeV/c^2. The Neural Network multivariate method is used to discriminate signal against comparatively large backgrounds. We measure a single top cross section of $3.04^{+0.57}_{-0.53}$ pb (stat. + syst.) and set a lower limit $|V_{tb}| > 0.78$ at the 95% confidence level, assuming $m_t = 172.5$ GeV/c^2. With a two-dimensional fit for σ_s and σ_t, we obtain $\sigma_s = 1.81^{+0.63}_{-0.58}$ pb and $\sigma_t = 1.49^{+0.47}_{-0.42}$ pb.

Acknowledgments

We thank the Fermilab staff and the technical staffs of the participating institutions for their vital contributions. This work was supported by the U.S. Department of Energy and National Science Foundation; the Italian Istituto Nazionale di Fisica Nucleare; the Ministry of Education, Culture, Sports, Science and Technology of Japan; the Natural Sciences and Engineering Research Council of Canada; the National Science Council of the Republic of China; the Swiss National Science Foundation; the A.P. Sloan Foundation; the Bundesministerium für Bildung und Forschung, Germany; the Korean World Class University Program, the National Research Foundation of Korea; the Science and Technology Facilities Council and the Royal Society, UK; the Institut National de Physique Nucleaire et Physique des Particules/CNRS; the Russian Foundation for Basic Research; the Ministerio de Ciencia e Innovación, and Programa Consolider-Ingenio 2010, Spain; the Slovak R&D Agency; the Academy of Finland; and the Australian Research Council (ARC).

---

[1] Nikolaos Kidonakis. Higher-order corrections to top-antitop pair and single top quark production. 2009. arXiv:0909.0037.
[2] Harald Grosse and Raimar Wulkenhaar. The beta-function in duality-covariant noncommutative phi**4 theory. *Eur. Phys. J.*, C35:277–282, 2004.
[3] T. Aaltonen et al. First Observation of Electroweak Single Top Quark Production. *Phys. Rev. Lett.*, 103:092002, 2009.
[4] V. M. Abazov and Abbott et al. Observation of single top-quark production. *Phys. Rev. Lett.*, 103(9):092001, Aug 2009.
[5] Johan Alwall et al. Is V(tb) = 1? *Eur. Phys. J.*, C49:791–801, 2007.
[6] Gregory Mahlon and Stephen J. Parke. Improved spin basis for angular correlation studies in single top quark production at the Tevatron. *Phys. Rev.*, D55:7249–7254, 1997.
[7] Gregory Mahlon and Stephen J. Parke. Single top quark production at the LHC: Understanding spin. *Phys. Lett.*, B476:323–330, 2000.
[8] Veronique Boisvert. Trigger Efficiencies for the High ET Central Electrons in Gen6. CDF Internal Note 7939, 2006.
[9] M. Franklin et al. Method 2 Backgrounds for 1.12 in fb^{-1} Lepton+Jets Analysis. CDF Internal Note 8766,, 2007.
[10] Jan Lueck Z. Wu, Dominic Hirschbuehl. POWHEG Signal Samples used in Single Top Analysis. CDF Internal Note 10325, 2010.
[11] T. Aaltonen et al. Observation of Single Top Quark Production and Measurement of —Vtb— with CDF. *Phys.Rev.*, D82:112005, 2010.
[12] The predicted cross section is calculated by taking average of cross section assuming top quark mass $m = 172$ GeV/c^2 and $m = 173$ GeV/c^2 using CTEQ pdf[1]. The number from [1] is for single top quark only. Since we don't select on the charge of the top quarks, we double those numbers as the single top and anti-top quark cross section as in Table. I. The cross sections and uncertainties are added linearly when combining the channels, as recommended in private communication with the author.
[13] η_{det} is defined as the pseudorapidity of the jet calculated with respect to the origin of the coordinate system, which is located in the center of the detector.